Water-Soluble Nonstoichiometric Complexes between Sodium Poly(styrenesulfonate) and Cetylpyridinium Chloride in Aqueous NaCl Solutions. A Static and Dynamic Light Scattering Study

ARTICLE *in* THE JOURNAL OF PHYSICAL CHEMISTRY B · MARCH 2011

Impact Factor: 3.3 · DOI: 10.1021/jp2008336 · Source: PubMed

THE JOURNAL OF PHYSICAL CHEMISTRY B

ARTICLE

pubs.acs.org/JPCB

Water-Soluble Nonstoichiometric Complexes between Sodium Poly(styrenesulfonate) and Cetylpyridinium Chloride in Aqueous NaCl Solutions. A Static and Dynamic Light Scattering Study

Simona Prelesnik,[†] Sergey Larin,[‡,§] Vladimir Aseyev,[‡] Heikki Tenhu,[‡] and Ksenija Kogej*[,†]

[†]Department of Chemistry and Biochemistry, Faculty of Chemistry and Chemical Technology, University of Ljubljana, P.O. Box 537, SI-1000, Ljubljana, Slovenia

[‡]Laboratory of Polymer Chemistry, Department of Chemistry, University of Helsinki, P.O. Box 55, FIN-00014 HU, Helsinki, Finland

Supporting Information

ABSTRACT: Complexes formed between a cationic surfactant cetylpyridinium chloride, CPC, and an anionic polyelectrolyte sodium poly(styrenesulfonate), NaPSS, in aqueous 0.1 M NaCl solutions were studied by static and dynamic light scattering and by ζ-potential measurements in a broad region of surfactant cation, CP^+, to polyanion, PSS^-, charge ratio, S/P. Two NaPSS samples were used, NaPSS-L with a lower molar mass, $M_w = 1.4 \times 10^5$ g/mol, and NaPSS-H with a considerably higher M_w ($= 2.6 \times 10^6$ g/mol), to elucidate the effect of the polyion chain length on the behavior of the aggregates. In the polyelectrolyte-rich regime ($S/P < 1$), CPPSS complexes are soluble up to rather high S/P values (around 0.72, irrespective of the polyion chain length), which is attributed to a specific interaction between the hydrophobic benzene groups on the polyion and the surfactant micelle, which leads to a less efficient charge screening. The addition of surfactant causes chain contraction. The obtained data suggest a pronounced effect of the NaPSS chain length on the structural properties of the CPPSS complexes. The CPPSS-L complexes are small and dense (the radius of gyration, R_g, is 7.3 nm at $S/P = 0.7$), and their shape is close to spherical. In contrast, the CPPSS-H complexes (R_g around 73 nm at $S/P = 0.7$) have no well-defined structure and reveal a stronger tendency toward intermolecular association when the nominal charge of the complex is reduced, although they remain pretty monodisperse. A model of a temporary network-like association in which surfactant micelles serve as cross-links for polyion chains is proposed to explain the behavior in CPPSS-H solutions. The forces responsible for such labile intermolecular association are weak, in contrast to strong specific interaction involved in the formation of the primary complex. The redissolution of the complex by adding excess surfactant ($S/P > 1$: the surfactant-rich regime) depends strongly on the polyion chain length and is a slow process, taking several days (CPPSS-L) or even weeks (CPPSS-H). It is achieved only at very high S/P values (around 240 and 2400 in the CPPSS-L and CPPSS-H cases, respectively) by hydrophobic binding of surfactant to the CPPSS complex. The predominating species in these solutions are free surfactant micelles. Similarly, a large excess of NaCl (almost 390 and 690 mol per 1 mol of CPPSS-L and CPPSS-H, respectively) is needed to disintegrate the stoichiometric CPPSS ($S/P = 1$) complex into free polyion chains and free surfactant micelles.

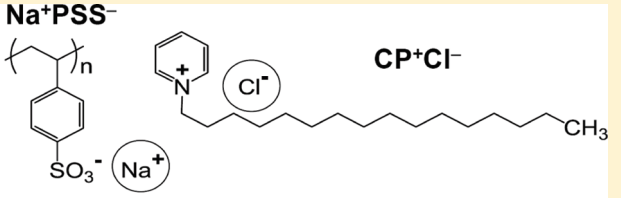

Soluble CP^+PSS^- Complexes in Aqueous 0.1 M NaCl

INTRODUCTION

Mixing oppositely charged polyelectrolytes and surfactants in aqueous solutions leads to an associative macro phase separation, which results in a dense precipitate (or coacervate) involving the polyelectrolyte−surfactant complex, PSC, and a dilute water phase (or supernatant) with excess low molar mass ions. This phenomenon is utilized in many applications, ranging from hair conditioners to the deposition of very compact layers of protective PSCs on solid surfaces. It has been well established by numerous studies throughout the years that the surfactant is assembled into polyelectrolyte-bound micelle-like aggregates in such complexes.[1−4]

We will describe the phase separation process in terms of the surfactant-to-polyelectrolyte charge ratio, S/P. Values of S/P below 1 refer to solutions with excess of the polyelectrolyte (the polyelectrolyte-rich regime), and those larger than 1 refer to solutions with excess of the surfactant (the surfactant-rich regime). The critical value of S/P at the onset of macro phase separation (designated as $(S/P)_1$) and its value at the upper border of the two-phase region (designated as $(S/P)_2$), where the precipitated PSC redissolves, depend on the structural features of the components involved, e.g., on the surfactant hydrocarbon tail length, the polyion charge density and flexibility, and the hydrophilic/hydrophobic character of functional groups attached to the polyelectrolyte chain.

Received: January 26, 2011
Revised: March 9, 2011

dx.doi.org/10.1021/jp2008336 | J. Phys. Chem. B XXXX, XXX, 000–000

In aqueous solutions of polyelectrolytes with hydrophilic side groups, e.g., in sodium hyaluronate, NaHy,[5] and sodium polyacrylate, NaPA,[6] solutions, the addition of a long alkyl chain surfactant cetyltrimethylammonium bromide, CTAB, induces precipitation already at $(S/P)_1 \approx 0.2$ or lower. On the other hand, shorter alkyl chain surfactants are less effective in precipitating the polymer.[5] Addition of dodecyltrimethylammonium bromide, DTAB, to NaHy induces precipitation at $(S/P)_1$ values higher than 1 (around 5), and in the case of octadecyltrimethylammonium bromide, OTAB, no precipitation is observed at all. Redissolution of the precipitated complex usually requires a large excess of surfactant, i.e., $(S/P)_2$ values considerably higher than 1.

The described behavior is quite general when the polyion contains hydrophilic side groups, as is the case with hyaluronate, Hy^-, and polyacrylate, PA^-. By contrast, complexes between poly(styrenesulfonate) anion, PSS^-, with hydrophobic benzene rings attached to the polymer backbone, and cationic surfactants are soluble in water up to rather high $(S/P)_1$ values (slightly below 0.72[7−12]), i.e., to a rather low nominal charge of the complex. Thus, perhaps contrary to expectations, the hydrophobic character of the PSS^- anion contributes to a better solubility of the PSC in the polyelectrolyte-rich regime. Besides, the $(S/P)_1$ value is not affected by the addition of NaCl at concentrations up to 0.1 M.[10,11] Binding studies in solutions of sodium poly(styrenesulfonate), NaPSS, and cetylpyridinium chloride, CPC, also show that CP^+ cations are almost quantitatively (100%) associated with the PSS^- anion, meaning that the free CP^+ concentration is virtually zero (well below 1×10^{-7} M)[10] and that the presence of free micelles may be excluded. Strong interactions between CP^+ and PSS^- were explained by considering simultaneous action of initial electrostatic binding and additional specific interaction between surfactant and the PSS^- chain, which is ascribed to the solubilization (inclusion) of the hydrophobic styrene groups of the PSS^- anion in the surface region of the polyion induced surfactant micelles.[7−13]

It has been found that such "mixed" micelles are smaller than the free ones and that the surfactant aggregation number, N_{agg}, depends strongly on the S/P value.[14] N_{agg} values in the range from around 30 (at $S/P \approx 0.2$) to around 78 (at $S/P \approx 0.65$) are reported in CTAB−NaPSS solutions,[14] whereas in polymer-free aqueous CTAB solution at a concentration of 40 mM N_{agg} is around 120.[15] Contrary to the CTAB−NaPSS case, the CTAB aggregation numbers in CTAB−NaPA solutions do not differ from those found for free CTAB micelles.[16] The comparatively small N_{agg} in the presence of NaPSS suggests that packing of surfactant into aggregates is restricted by the presence of the solubilized styrene group, whereas this is not the case with NaPA. In addition, the specific way of PSS^- binding to the micelle may result in a less efficient screening of the micellar charge due to spatial constraints. Thus, complexes may be locally overcharged and this overcharging enables them to resist precipitation. The described behavior in solutions of surfactants and homopolymers may help in understanding the phenomena observed in various more complex polyelectrolyte−surfactant mixtures, e.g., in mixtures of copolymers or comb-type copolymers and surfactants.[17−22]

The purpose of this study is to investigate the molecular characteristics of the soluble complexes between CPC and NaPSS, denoted herein as CP^+PSS^- or shortly CPPSS, below and in the vicinity of the precipitation zone at $(S/P)_1$ and above the redissolution limit at $(S/P)_2$ using static light scattering, SLS, and dynamic light scattering, DLS, and in addition to these zeta (ζ) potential measurements. Simultaneous SLS and DLS measurements in polymer−surfactant mixtures can provide important structural information about such systems.[23−28] Our aim is to answer the following questions: (i) What is the influence of the specific interaction between PSS^- and the micellized surfactant on molecular parameters of CPPSS complexes? (ii) How does the degree of complexation affect the overall charge of the complex, and in this connection why is the complex soluble in a rather broad region of S/P values in the polyelectrolyte-rich regime? (iii) Do these complexes involve one (intra PSCs) or several (inter PSCs) polyion chains; how polydisperse are they? (iv) What is the effect of the polyion chain length (degree of polymerization) on structural characteristics? In order to elucidate the last point, two NaPSS samples with low polydispersities that differed widely in their molar mass values were employed. The CPPSS complexes were studied in the presence of 0.1 M NaCl at 25 °C and below the so-called overlap concentration, c^*, i.e., in rather dilute solutions; the total solute concentrations did not exceed 1 wt %. The high salt concentration was chosen in order to avoid bimodality that is usually observed in correlation functions of polyelectrolyte solutions at low ionic strength. Much confusion prevails in the literature in relation to the origin of this bimodality.[29−32] Authors associate the biexponential (or perhaps multiexponential) decays either with the appearance of a new (extraordinary) "phase" in addition to the ordinary one (i.e., single polyelectrolyte chains)[29] or with so-called fast and slow diffusive modes of polyelectrolyte chains, which are attributed to collective motions of individual polyion chains and to multi macroion domain formation, respectively.[30,31] Investigation of these phenomena is out of the scope of this paper.

EXPERIMENTAL SECTION

Materials. *N*-Cetylpyridinium chloride, CPC, (Kemika, Zagreb, Croatia) was purified by repeated recrystallization from acetone and dried under vacuum at 50 °C. NaCl (Titrisol, Merck KGaA) was used for the preparation of a 0.1 M aqueous solution. Two samples of poly(styrenesulfonic acid) sodium salts, NaPSS, from Fluka were used. They were both GPC standards with rather different weight-average molar mass values, M_w. The sample designated as NaPSS-L had a lower M_w (=1.52×10^5 g/mol), and the sample designated as NaPSS-H had a considerably higher M_w (=2.26×10^6 g/mol). The polydispersities, M_w/M_n, of parent polystyrenes, as given by the producer, were 1.03 and 1.02 for low and high molar mass samples, respectively, the degree of sulfonation was 1, and the polydispersity of the sulfonated samples was below 1.2 in both cases. The NaPSS samples were used as received.

Preparation of Solutions. All solutions for light scattering, LS, measurements were prepared in aqueous NaCl solution with a concentration of 0.1 mol/L (=M). CPC-free NaPSS solutions (S/P = 0) and pure (NaPSS-free) CPC solutions (S/P undefined) were prepared by simply dissolving solid NaPSS or solid CPC in 0.1 M NaCl. The stock solutions were kept at gentle stirring for 24 h and then diluted with 0.1 M NaCl. For the mixed CPPSS solutions the preparation protocol was the following. First, NaPSS and CPC stock solutions of known concentrations, c, were prepared in water, allowing enough time for the dissolution of the solid samples. A calculated amount of the CPC solution was very slowly added to the NaPSS solution under vigorous stirring so that a desired S/P ratio was achieved. Gentle stirring or shaking was thereafter continued for 24 h to attain equilibrium. Upon binding of CPC by NaPSS the nonstoichiometric

dx.doi.org/10.1021/jp2008336 |J. Phys. Chem. B XXXX, XXX, 000–000

CPPSS complex ($S/P < 1$) is formed and an equivalent amount of low molar mass counterions Na^+ and Cl^- is released into the solution. The amount of NaCl resulting from this was calculated by taking into account 100% binding of CP^+ ions by PSS^- anion, which was proven previously by potentiometric measurements.[9] At the end, a calculated amount of 1 M NaCl was added to adjust its final concentration in solution to 0.1 M. Stock solutions, prepared in this way, were successively diluted with 0.1 M NaCl. Prior to measurements, solutions were kept at gentle agitation for 24 h at ambient temperature. In this way, CPPSS complex solutions with the following S/P values were prepared: (a) S/P = 0.25, 0.50, and 0.70 in the case of NaPSS-L (these samples are designated as CPPSS-L) and (b) S/P = 0.25, 0.45, 0.50, 0.60, and 0.70 in the case of NaPSS-H (these samples are designated as CPPSS-H). Even after prolonged storage (for several months), the appearance of these mixed CPPSS solutions did not change. They remained perfectly clear. LS measurements performed immediately after solution preparation and a few months afterward showed no change in particle sizes and in LS intensity.

CPPSS solutions were probed also in the one-phase region above $(S/P)_2$ with a large excess of added surfactant. Since the total solute concentrations in this regime were very high (up to ~25 wt %), for unequivocal application of the LS techniques, these investigations were performed only by DLS for one S/P value for each PSS sample. In addition, clear (one-phase) CPPSS complex solutions with S/P = 1 (the stoichiometric complex) were prepared in the presence of a large excess of NaCl and were also investigated by DLS.

Methods. *Light Scattering Measurements.* Methodological aspects of DLS and SLS can be found elsewhere,[33,34] and the detailed aspects of the data analysis used in this paper are presented in the Supporting Information. All LS studies were performed at 25 °C. Solutions were filtered directly into the measuring cell through hydrophilic Millex-HV filters with a pore size of 0.20 μm and a diameter of 13 mm. In the case of CPC or NaCl solubilized complexes, filters with a larger pore size (0.45 μm) were used. The samples were allowed to equilibrate for 30 min before measurement. Constant intensity of the light scattered at 90° was used as a criterion that the solution was properly equilibrated. Measurements were performed in cylindrical quartz sample cells with a total volume of 2.7 mL. Normally, a cell was filled with around 0.8 mL of the solution.

DLS and SLS measurements were conducted using two LS setups: (1) The first one was composed of a Brookhaven Instruments BI-200SM goniometer, a BIC-TurboCorr digital pseudo-cross-correlator, and a BI-CrossCorr detector, including two BIC-DS1 detectors; pseudo-cross-correlation functions of the scattered light intensity were collected with the self-beating method;[35] a Sapphire 488-100 CDRH laser from Coherent GmbH operating at λ_o = 488 nm and power adjusting in the range from 10 to 50 mW was used as the light source. (2) The second one, a three-dimensional (3D) LS spectrometer from LS Instruments GmbH (Fribourg, Switzerland), was used in the 3D cross-correlation mode;[36] two coherent incident light beams were generated with a 20 mV He−Ne laser (Uniphase JDL 1145P), operating at λ_o = 632.8 nm. The instrument is equipped with a laser attenuation system combined with an online incident laser intensity measurement that allows for the normalization of the static LS data.

Scattered light was collected in the angular range between 30 and 150°. Correlation functions of the light intensity scattered at an angle θ, $G_2(t)$, were recorded simultaneously with the integral time average intensities, $I(\theta) \equiv I(q)$, where q (=$(4\pi n_o/\lambda_o)$ $\sin(\theta/2)$) is the scattering vector and n_o is the refractive index of the medium. Intensities measured in counts of photons per second, cps, were normalized with respect to the Rayleigh ratio of toluene. In order to determine the weight-average molar mass of the scattering objects, M_w, and the radius of gyration, R_g, we used the Zimm double extrapolation method.

In the DLS experiment, $G_2(t)$ can be converted into a correlation function of the scattered electric field, $g_1(t)$, using the Siegert's relationship.[33,34] For monodisperse particles small in diameter compared to the wavelength of light as well as for hard spheres of any size, the relaxation (or decay) time of $g_1(t)$, τ, is related to the relaxation rate of $g_1(t)$, Γ, and the translation diffusion coefficient, D, by the relationship

$$g_1(t) = e^{-t/\tau} = e^{-\Gamma t} = e^{-Dq^2 t} \quad \text{and}$$
$$\Gamma = \tau^{-1} = Dq^2 \tag{1}$$

The hydrodynamic radii of particles are then obtained from the diffusion coefficient, D, via the Stokes−Einstein equation

$$R_h = \frac{kT}{6\pi\eta_o D} \tag{2}$$

where k is the Boltzmann constant, T is the absolute temperature, and η_o is the solvent viscosity.

For particles with moderately broad size distributions, a multiexponential fit of either $G_2(t)$ or $g_1(t)$ can be used. Thus, we collected from 5 to 10 intensity correlation functions. Each curve was analyzed independently and compared with the averaged curve to ensure accuracy of the mathematical solution provided by the inverse Laplace transform program CONTIN.[37] Mean peak values of the size distributions, obtained at fixed q and c, were used to estimate the apparent hydrodynamic radii, R_h^{app}. The true hydrodynamic radius, R_h, as well as the true radius of gyration, R_g, were then obtained by extrapolating to q = 0 and c = 0. Decay rates of $g_1(t)$ were calculated from R_h^{app}.

A note on the calculation of the concentration, c (in mg/mL), in the light scattering expression for Kc/R_θ and in the relationship for the specific refractive index increments, dn/dc, is necessary. The calculation is straightforward for pure NaPSS samples (via the molar mass of the monomer unit: M_{NaSS} = 206.2 g/mol), whereas for the nonstoichiometric CPPSS complexes, the value of the molar mass of the polyelectrolyte's monomer unit, denoted as M_{PSC} (where the subscript PSC stands for the polyelectrolyte−surfactant complex), depends on the amount of bound CP^+. This value was obtained in the following way:

$$M_{PSC} = \frac{S}{P}M_{CPSS} + \left(1 - \frac{S}{P}\right)M_{NaSS} \tag{3}$$

M_{CPSS} (=487.7 g/mol) in eq 3 is the monomer molar mass of the stoichiometric CPPSS complex.

Refractive Index Increment Measurements. A Wyatt Optilab rEX differential refractometer (λ_o = 632.8 nm) was used to determine the dn/dc for CPPSS solutions at constant S/P values. In these experiments, the NaPSS-L sample was used, and concentrations of pure NaPSS and of nonstoichiometric CPPSS complexes were between 0.2 and 9 mg/mL, whereas those of CPC were between 3.0 and 30.0 mg/mL. Within experimental error, dn/dc values for all S/P ratios studied, as well as for pure NaPSS and CPC solutions, were equal. Thus, an average value of

dx.doi.org/10.1021/jp2008336 |J. Phys. Chem. B XXXX, XXX, 000–000

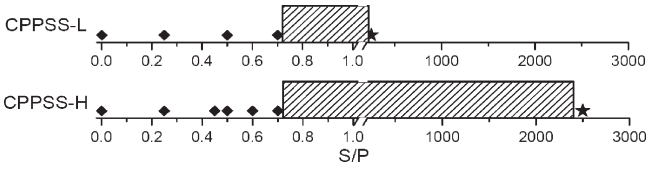

Figure 1. One-phase (unshaded areas) and two-phase regions (shaded areas) observed for the CPPSS-L and CPPSS-H complex solutions in 0.1 M NaCl in dependence on the S/P mixing ratio. Symbols indicate the one-phase solutions of the complexes that were analyzed by LS: the diamonds show the polyelectrolyte-rich one-phase samples ($S/P < 0.72$) and the stars show the surfactant-rich one-phase samples ($S/P \approx 250$ and 2500 for CPPSS-L and CPPSS-H, respectively).

$dn/dc = 0.164 \pm 0.003$ mL/g was used in all calculations. This value agrees with the available literature data. The dn/dc for NaPSS is reported to be in range from 0.152 to 0.198 mL/g,[38,39] depending on the wavelength of the laser light and on the type and concentration of added salt. For pure CPC, dn/dc = 0.19 mL/g was previously determined in aqueous 0.2 M NaCl at λ_o = 436 nm.[38] The values, determined in this work for CPC and NaPSS in aqueous 0.1 M NaCl and at λ_o = 633 nm, are dn/dc = 0.1622 and 0.1627 mL/g. Data for complexes and further experimental details on dn/dc measurements are reported in the Supporting Information and in Figure 1S in the Supporting Information.

Zeta-Potential Measurements. Zeta (ζ) potential was measured with a Zetasizer Nano-ZS ZEN3600 from Malvern Instruments Ltd. The Zetasizer is equipped with a 4 mW He−Ne laser operating at λ_o = 633 nm. Measurements of ζ were performed at $\theta = 17°$. Simultaneously, R_h was determined at the backscattering angle of $\theta = 173°$. In this case, data were collected at a constant monomolar concentration (monoM = moles of monomer units per volume) of the polyelectrolyte (0.03 monoM for CPPSS-L and 0.01 monoM for CPPSS-H) and at several S/P values ranging from 0 to 0.7. No precipitation has been observed during or after the measurements.

RESULTS AND DISCUSSION

Solubility of the CPPSS Complex. Figure 1 shows the one- and two-phase regions (the precipitated complex in equilibrium with the solvent) determined in 0.1 M NaCl for CPPSS-L and CPPSS-H solutions. The symbols indicate S/P values for the systems that were subsequently analyzed by LS. One can see that the isotropic one-phase region extends up to $(S/P)_1 = 0.72$ and above $(S/P)_2 \approx 240$ or 2400 for CPPSS-L and CPPSS-H, respectively. The two-phase region is very broad, in particular in the CPPSS-H case. Interestingly, the S/P value at the onset of precipitation in 0.1 M NaCl is the same as the one determined in water[11] and it does not depend on the molar mass of NaPSS, whereas the redissolution boundary is strongly affected by the polyion chain length. At the same time, precipitation at $(S/P)_1$ is a fast process for both CPPSS-L and CPPSS-H, whereas redissolution depends strongly on the polyion chain length and is a slow process, taking several days (CPPSS-L) or even weeks (CPPSS-H).

We first discuss the solubilization by excess CPC. The total mass concentration of the isotropic solutions of the redissolved CPPSS complexes (indicated by stars in Figure 1) was around 150 and 225 mg/mL in CPPSS-L and CPPSS-H solutions, respectively. Under these conditions, the total CPC concentration

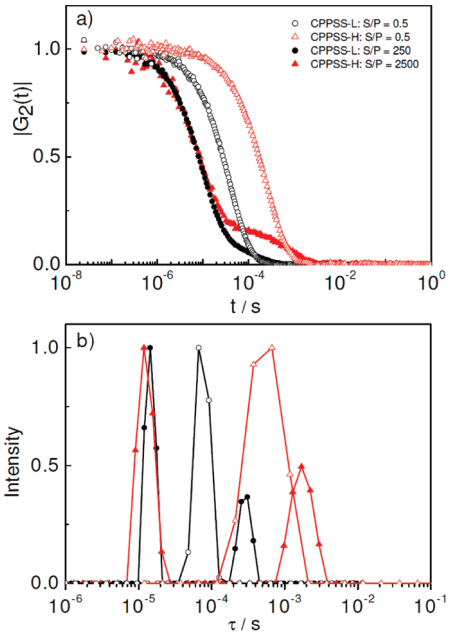

Figure 2. (a) Normalized correlation functions of the scattered light intensity, $|G_2(t)| = (G_2(t) - G_2(\infty))/(G_2(0) - G_2(\infty))$, obtained at θ = 90° for the CPPSS-L (black circles) and CPPSS-H (red triangles) complexes: S/P = 250 (filled circles) and 2500 (filled triangles) in 0.1 M NaCl. For comparison, CPPSS complexes with S/P = 0.5 for CPPSS-L (open circles) and CPPSS-H (open triangles) are included. (b) The corresponding distributions of relaxation time, τ (symbols the same as in (a)).

in solution (0.43 and 0.64 M) is considerably higher than its critical micelle concentration, cmc (=3.8×10^{-5} mol/L in 0.1 M NaCl at 25 °C[7]), meaning that free CPC micelles are present. The resulting solutions were analyzed by DLS at three angles (θ = 45, 90, and 135°). The correlation functions were clearly bimodal (see Figure 2a, filled symbols). The corresponding relaxation time distributions plotted in Figure 2b (filled symbols and solid lines) show a fast relaxation mode and an additional considerably slower relaxation mode. The fast mode is attributed to free CPC micelles and the slow one is attributed to the solubilized complex. Although the complexes are not many in number, they significantly contribute to the intensity of scattered light (the relative amplitude of the larger particles is up to 50%).

Figure 2b also gives the relaxation time distribution functions for the CPPSS-L and CPPSS-H complexes with S/P = 0.5. It can be seen that the latter two distributions are monomodal with a single peak positioned between the peaks in the redissolved CPPSS systems. On the basis of these results it was concluded that the predominant species in solutions of solubilized complexes in the surfactant-rich regime (high S/P values) are free CPC micelles accompanied by a small amount of the solubilized complexes with hydrophobically bound surfactant. Estimation of particle size in these solutions is not straightforward because the viscosity of the medium as well as the refractive index of solutions with such high mass concentrations of solutes can differ significantly from their values in dilute solutions. Nevertheless, a rough estimate of the apparent R_h value from the measurement at 90° using the η_o value for water (eq 2) is the following: R_h is around 1.24 and 1.1 nm for free CPC aggregates and around 20 and 150 nm for solubilized polyelectrolyte−surfactant complexes in CPPSS-L and CPPSS-H solutions, respectively (note

dx.doi.org/10.1021/jp2008336 |J. Phys. Chem. B XXXX, XXX, 000–000

Table 1. Physical Parameters Obtained at 25 °C from Light Scattering Measurements on CPPSS-L and CPPSS-H Complexes at Different S/P Ratios in Aqueous 0.1 M NaCl

complex	S/P	M_w (g/mol)	A_2 (mL mol g^{-2})	R_g (nm)	R_h (nm)	R_g/R_h	c^* [a] (mg/mL)
CPPSS-L	0	1.39×10^5	1.06×10^{-3}	14.9	10.4	1.4	16
	0.25	1.85×10^5	3.4×10^{-4}	14.5	9.0	1.6	23
	0.5	2.85×10^5	6×10^{-5}	9.2	7.7	1.2	145
	0.7	3.53×10^5	-1×10^{-8}	7.3	7.8	0.9	355
CPPSS-H	0	2.57×10^6	1.5×10^{-4}	90.2	69.5	1.3	2
	0.25	4.67×10^6	6×10^{-5}	77.5	65.5	1.2	4
	0.45	6.44×10^6	1×10^{-5}	65.5	60.3	1.1	9
	0.5	6.73×10^6	6×10^{-6}	61.4	59.1	1.0	12
	0.6	8.11×10^6	3.6×10^{-6}	67.1	60.1	1.1	11
	0.7	9.34×10^6	3×10^{-6}	72.7	61.0	1.2	10

[a] The overlap concentration, c^*, is estimated using the radius of gyration, R_g.

that the total concentration of CPC is different in CPPSS-L and CPPSS-H solutions as well as the total mass concentration of solutes; see above). For comparison, the zero concentration R_h values of the surfactant-free NaPSS-L (NaPSS-H) and of the CPPSS-L (CPPSS-H) complexes with $S/P = 0.7$ (the polyelectrolyte-rich regime) are around 10 (70) nm and 8 (60) nm, respectively (see the data reported in Table 1).

On the basis of these results we propose the following dissolution mechanism of the precipitated CPPSS complex by excess surfactant. The stoichiometric CPPSS complex is strongly stabilized by the specific interaction between benzene moieties and the CPC micelle, which hinders the reorganization of the polyion-bound micelles required in order to include excess surfactant. Thus, adding excess surfactant first leads to the formation of free CPC micelles in equilibrium with the solid complex. Nevertheless, at sufficiently high CPC concentrations, surfactant binding to the hydrophobic complex (with hydrocarbon tails oriented toward the complex) slowly increases as well to the extent that complexes become net positively charged and thus soluble in the aqueous medium. Note that the average value of the ζ-potential measured in these solutions was around +30 and +27 mV for CPPSS-L and CPPSS-H, respectively. A large excess of CPC is needed to achieve this stage, and the particles present in solution are free CPC micelles and CPPSS complexes with a layer of hydrophobically bound surfactant. A similar mechanism has been proposed for other hydrophobic polyelectrolytes.[40,41] Finally, our results also show that the redissolution of the complex depends on the polyion molar mass (chain length). Complexes involving longer chains are more difficult to solubilize. Certainly, a larger amount of CPC is needed for the formation of a solubilizing layer around a larger particle (cf. CPPSS-H complex). However, this cannot be the only reason for the huge difference in solubilities of CPPSS-L and CPPSS-H complexes. Other factors, e.g., differences in conformation or intermolecular association, may play an even more important role. This issue will be discussed below.

It is also expected that PSCs formed between oppositely charged polyions and surfactant ions can be decomposed by adding a large excess of an inert electrolyte as a consequence of the electrostatic screening. In our case, the effect of NaCl on the dissolution of the complex was studied. The CPPSS complex ($S/P = 1$) was preformed in 0.1 M NaCl, and then NaCl concentration was gradually increased by adding 2 M NaCl. After prolonged mixing at 25 °C, the solution became clear at around 0.88 M NaCl in the CPPSS-L case and at around 1.12 M NaCl in the CPPSS-H case, which corresponds to 386 and 690 molar excess of NaCl over monomer units in CPPSS, respectively. The solubilized samples were analyzed by DLS. The scattering from these solutions was very strong, as was the one from pure NaPSS solutions at the same salt concentrations. On the other hand, scattering from pure CPC in 1 M NaCl (an intermediate between 0.88 and 1.12 M NaCl) at concentrations comparable to those in CPPSS solutions was extremely weak.

The relaxation time distribution functions resulted in $R_h = 9$ and 55 nm for CPPSS-L and CPPSS-H solutions, respectively (both at $\theta = 90°$). These R_h values are close to those obtained in NaPSS-L and NaPSS-H solutions with no added CPC and at the same salt concentrations ($R_h \approx 8.5$ nm for NaPSS-L in 0.88 M NaCl and $R_h \approx 54.3$ nm for NaPSS-H in 1.12 M NaCl). The hydrodynamic radius of free CPC micelles in 1 M NaCl was estimated to be around 3 nm (measured in a 0.005 M CPC solution). It was thus concluded that the above R_h values correspond to free polyion chains that are strongly contracted due to high salt concentration, whereas the scattering originating from free CPC micelles, which accompany the chains, is extremely weak and is not manifested in size distributions obtained for NaCl solubilized CPPSS complexes.

The solubilization experiments of CPPSS with NaCl thus show that the stoichiometric complex between PSS^- anion and CP^+ micelles is disintegrated into free micelles and free polyion chains at sufficiently high electrolyte concentrations. On first thought this is expected due to the electrostatic screening effect of the simple salt. However, the required NaCl concentration for CPPSS complex decomposition is much higher in comparison with systems where electrostatic force is the only (or main) attractive force between polyion chains and cationic surfactants. For example, Hansson and Almgren[16] have demonstrated that a NaPA−CTAB solution with a NaPA concentration of 0.15 *m* remains a single homogeneous phase for NaBr concentrations higher than 0.34 *m*. The corresponding molar excess of NaBr relative to charged groups of NaPA in this case is only around 2.5. In the same work[16] it is reported that a homogeneous one-phase region in the NaPSS−CTAB system is achieved at 0.5 *m* NaBr (or around 3.7 molar excess of NaCl relative to polyion concentration). Clearly, a much larger salt excess is needed to dissolve the CPPSS complex. First, the comparison with the NaPA−CTAB case confirms the great significance of additional specific polyion bridging forces in complexes with poly(styrenesulfonate).

dx.doi.org/10.1021/jp2008336 |J. Phys. Chem. B XXXX, XXX, 000–000

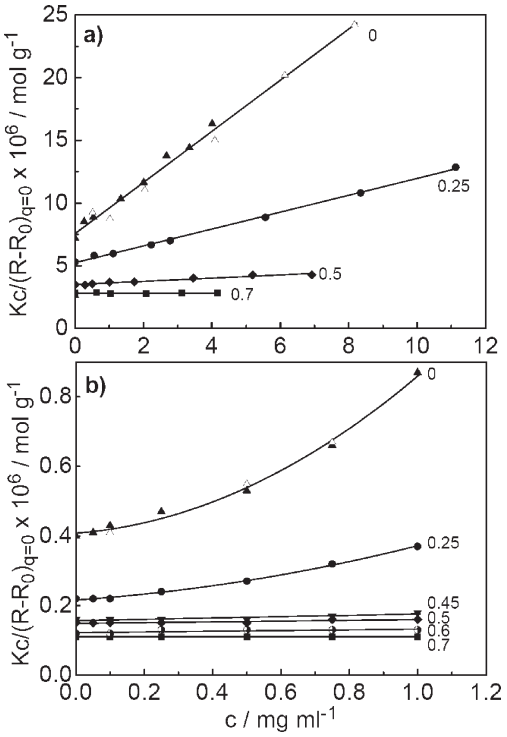

Figure 3. Concentration dependence of the inverse reduced intensity of scattered light, $Kc/(R - R_o)_{q=0}$, where K is the optical constant, for (a) CPPSS-L (S/P = 0, 0.25, 0.5, and 0.7) and (b) CPPSS-H complexes (S/P = 0, 0.25, 0.45, 0.5, 0.6, and 0.7). Data for pure polyelectrolyte (S/P = 0) were obtained using both LS instruments (see Experimental Section): 3D LS spectrometer (filled triangles) and Brookhaven Instruments (open triangles).

In addition, the comparison with the NaPSS−CTAB case suggests that the nature of surfactant plays an important role as well. Although there is a difference in molar mass of the NaPSS sample in ref 16 (M_w = 90 000 g/mol) and in polyion concentration in comparison with our study, the NaPSS complex with CPC seems to be considerably more stable than the one with CTAB. This observation may be attributed to the aromatic pyridine ring in CPC.

Basic Characterization. Subsequent LS measurements were focused on CPPSS complexes with S/P values below 0.72. This is the region where nonstoichiometric complexes dominate the scattering and the S/P ratio in the complexes can be varied in a controllable way. We have performed DLS and SLS experiments simultaneously at a fixed S/P ratio in dependence on the total mass concentration of the complex.

First, the molar mass values of the NaPSS samples (S/P = 0) were determined in 0.1 M NaCl. The data obtained from both LS setups (see the Experimental Section) agreed within the experimental error (see the data points in Figure 3), and the determined M_w values were in good agreement with those provided by the supplier (compare the M_w values reported in the Experimental Section with the data in Table 1).

Special care was taken to perform all LS studies in dilute solutions, i.e., for sample concentrations well below the overlap concentration, c^*. Assuming a uniform distribution of the polymeric material within a scattering particle, c^* is obtained from $c^* = M_w/[N_A(4/3)\pi R_g^3]$, where N_A is the Avogadro constant. By taking into account the determined R_g values for both NaPSS samples, the dilute concentration region is c < 16 mg/mL for NaPSS-L and c < 2 mg/mL for NaPSS-H. The c^* values increase with increasing S/P (see the last column in Table 1). The data collected for complexes consisting of NaPSS-L indicate that the measurements were indeed performed well below the c^*, and thus the concentration dependence of $Kc/(R - R_o)_{q=0}$ was linear for all S/P values investigated (Figure 3a). The data for NaPSS-H were also collected at concentrations below c^* (c < 1 mg/mL); nevertheless, some $Kc/(R - R_o)_{q=0}$ vs c dependences are curved in this case (see Figure 3b, curves for S/P = 0 and 0.25). This behavior is typical for polyelectrolytes with high molar mass values in the vicinity of c^* and is due to the long-range Coulomb interactions between highly charged and long polyions. Increasing the S/P values for CPPSS-H complexes results in a linear $Kc/(R - R_o)_{q=0}$ vs c dependence due to the fact that the charge of the complex decreases as more and more surfactant is bound to the polyion (see curves for $S/P \geq 0.45$ in Figure 3b). A second order polynomial fit was used to estimate the second osmotic virial coefficient, A_2, and M_w in the case of CPPSS-H solutions with S/P = 0 and 0.25, whereas a linear fit was applied to other S/P values.

Light Scattering from CPPSS Complex Solutions. At sufficiently low concentrations (c < 0.25 mg/mL for CPPSS-H and c < 11 mg/mL for CPPSS-L), all $Kc/(R - R_o)_{q=0}$ vs c dependences are linear and distributions of the apparent hydrodynamic radius, R_h^{app}, are monomodal for both polymers. Besides, the mean hydrodynamic radii do not depend on the way in which the complexes were prepared, i.e., either by dilution of the stock solution or by direct preparation of solutions with a predefined concentration. This suggests that the CPPSS particles are equilibrium structures.

An example of the intensity correlation function normalized between 1 and 0, $|G_2(t)| = (G_2(t) - G_2(\infty))/(G_2(0) - G_2(\infty))$, the corresponding electric field correlation function, the ln $g_1(t)$ vs t plot, and the calculated distributions of R_h^{app} are reported in Figure 4 for complexes with S/P = 0.5 and c = 0.25 mg/mL (CPPSS-H case; Figure 4a) and c = 0.29 mg/mL (CPPSS-L; Figure 4b). For all solutions, the dependence of the decay rate Γ vs q^2 passes through the origin of coordinates (see examples in Figure S3 in the Supporting Information), thus representing a diffusive process. However, in contrast to the perfectly linear dependence for CPPSS-L, the Γ vs q^2 for CPPSS-H shows positive deviations from linearity in the range of large q. This, in combination with a weaker angular dependence of R_h^{app}, implies a moderate polydispersity of the scattering CPPSS-H particles. However, one should keep in mind that this estimation of polydispersity is based on the size (not mass) measurements. For a long highly swollen chain with a low polydispersity index ($=M_w/M_n \approx 1$) as is the case with our NaPSS-H, a reasonably broad size distribution is typical and extrapolation of R_h^{app} to zero angle correctly describes the scatterers.

All correlation curves for S/P ratios up to 0.7 resembled the ones reported in Figure 4 and thus indicate that no free micelles are present in solutions of CPPSS complexes; i.e., almost all surfactant is associated with the polyion. The calculated R_h^{app} distributions from the CPPSS solutions showed no small objects in addition to either of the complexes. The absence of free micelles was established also previously by using several other experimental techniques,[7−12] which showed that the very small amount of free surfactant in PSS^- solutions is present in the monomer form (the concentration of free surfactant is below 1×10^{-7} M,[10] which is considerably lower than the cmc value).

dx.doi.org/10.1021/jp2008336 |J. Phys. Chem. B XXXX, XXX, 000–000

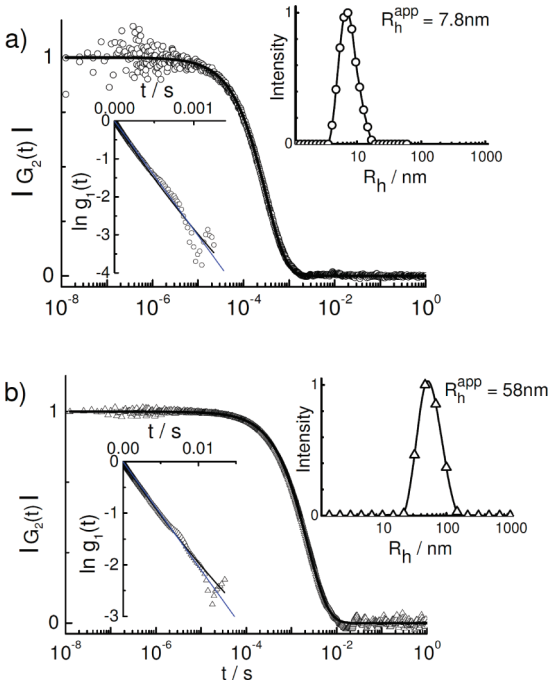

Figure 4. Normalized intensity correlation functions, $|G_2(t)| = (G_2(t) - G_2(\infty))/(G_2(0) - G_2(\infty))$, of light scattered at $\theta = 30°$ by the CPPSS complexes with $S/P = 0.5$ in aqueous 0.1 M NaCl: (a) CPPSS-L with c = 0.29 mg/mL and (b) CPPSS-H with c = 0.25 mg/mL. The data were collected using the 3D DLS−SLS spectrometer. The solid line shows the multiexponential fit. The corresponding distribution of the apparent hydrodynamic radius, R_h^{app}, is presented in the upper inset. The other inset shows the equivalent correlation function of the scattered electric field, $g_1(t)$, plotted as $\ln g_1(t)$ versus t. As can be seen, the $\ln g_1(t)$ vs t curve only slightly deviates from linearity for both CPPSS-H and CPPSS-L, i.e., from a single exponential decay. The straight blue line is a guide for the eyes and evidences the narrow monomodal size distribution of particles.

Therefore, the occurrence of free CPC micelles was neglected in our studies.

All molecular parameters for CPPSS-L and CPPSS-H complexes obtained from LS measurements are reported in Table 1. It can be seen that M_w increases (see also Figure 3), whereas R_g and R_h decrease with increasing S/P in both cases. This indicates that the PSCs are becoming denser as the system approaches the phase separation limit. The contraction (or compaction[28]) of the polyion is actually very strong. Binding of surfactant by the polyion with no change in polyion conformation should lead to an increase in size; however, R_g decreases from around 15 nm (90 nm) for pure NaPSS-L (NaPSS-H) to around 7 nm (at S/P = 0.7) and 60 nm (at S/P = 0.5) for CPPSS-L and CPPSS-H, respectively. This behavior is very different from the one noticed in complexes with rigid polyions. For example, in mixed solutions of DTAB with short DNA chains containing between 180 and 220 base pairs,[26] the effective diameter of complexes at finite concentration and for degrees of surfactant binding below 1 (the polyelectrolyte-rich regime) increased with increasing surfactant binding. Furthermore, Dias et al.[28] have demonstrated the existence of two populations in solutions of long DNA molecules (164 kbp) and CTAB: in a rather broad region of S/P ratios between 4 and 20 (the surfactant-rich regime), extended DNA coils coexisted with compacted DNA molecules. These results indicate that a large excess of positive charge is required to compact DNA, in contrast to the PSS case.

Increasing the fraction of CPC in both complexes up to S/P = 0.5 also results in narrowing of the apparent size distributions measured at each angle. Moreover, the Γ vs q^2 dependence passes through zero and becomes linear with increasing S/P up to 0.5. However, the slope of the R_h vs q^2 dependence remains negative at any S/P. In the vicinity of S/P = 0.5, CPPSS complexes are sufficiently hydrophobic and have rather high packing densities, thus suggesting a roughly spherical shape of the complexes. The negative slope proposes that the scattering particles are somewhat polydisperse. This polydispersity is not apparent as it was for the loose NaPSS coils and results from a variety of CPPSS architectures. Therefore, the extrapolation of R_h to $\theta = 0°$ primarily describes the fraction of the large scatterers. R_g was estimated using the initial slope of the q^2 vs LS intensity and thus describes the same large particles.

One should also note that, in DLS experiments, the translational diffusion coefficient, D ($=\Gamma q^{-2}$), is measured rather than R_h. D is concentration dependent even if the actual size of the scattering particles is constant. This is especially pronounced for strongly interacting polymers. Thus, R_h^{app} measured for both NaPSS samples at $S/P = 0$ decreases upon dilution, whereas no concentration dependence of R_h^{app} has been detected for the complexes with high S/P values where A_2 approaches zero.

Simultaneously with the decrease of the particle size, the thermodynamic quality of the solvent decreases. Thus, as is expected, the second osmotic virial coefficient, A_2, is positive and is considerably higher for NaPSS-L than for NaPSS-H. A_2 decreases steeply from rather high values for pure NaPSS-L to almost zero at $S/P \geq 0.5$, which agrees with the increase in packing density. The apparent packing density, ρ, of PSC material within a particle of radius R_g numerically coincides with c^* and is presented in Table 1 and plotted in Figure 5.

It appears from the data in Figure 5 that structures of PSCs formed by NaPSS-L and NaPSS-H are different. Thus, the largest value of the shape parameter, i.e., the R_g/R_h ratio, for CPPSS-L is found at S/P = 0.25 (R_g/R_h = 1.6) and is characteristic for a monodisperse random coil in a solvent whose quality is between θ conditions and a good solvent.[33] The shape parameter of CPPSS-L decreases gradually at higher S/P ratios and reaches its lowest value of R_g/R_h = 0.9 at S/P = 0.7. The latter R_g/R_h value is close to 0.78, known for a homogeneous nondraining sphere,[33] and denotes a highly compact character of the complexes with shorter PSS^- chains just before they precipitate from the aqueous medium. This justifies the use of the term "compaction"[28] to describe the change in polyion conformation upon surfactant binding.

The dependence of R_g/R_h on S/P for long-chain complexes (CPPSS-H) is weak. In the region $S/P \leq 0.5$ values are lower in comparison with short-chain complexes (CPPSS-L). They decrease smoothly from R_g/R_h = 1.3 at S/P = 0 to the minimum value of R_g/R_h = 1 at S/P = 0.5 and increase again for $S/P > 0.5$ to reach R_g/R_h = 1.2 at S/P = 0.7, which is close to the initial value. Lower R_g/R_h values at $S/P < 0.5$ indicate a more coiled (less expanded) form of the CPPSS-H complex, which can be expected due to considerably longer polyion chains. Shorter polyion chains turn out to be more expanded, especially with some bound surfactant aggregates (cf. the CPPSS-L case with S/P = 0.25). This may be easily visualized by the pearl necklace model: pearls knitted on a thread make the thread locally more extended, but with sufficiently long threads coils are easily

dx.doi.org/10.1021/jp2008336 |J. Phys. Chem. B XXXX, XXX, 000–000

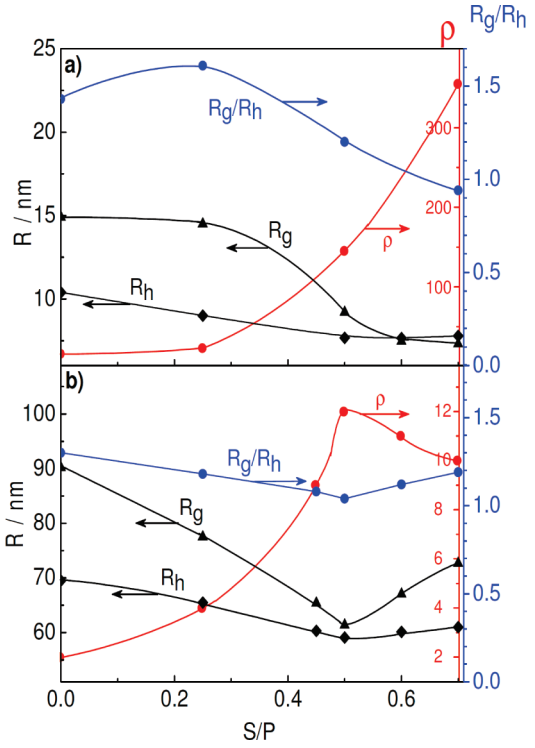

Figure 5. Concentration dependences of R_h (black filled diamonds), R_g (black filled triangles), R_g/R_h (blue filled circles), and the apparent packing density, ρ (red filled circles), for (a) CPPSS-L and (b) CPPSS-H complexes. Data are obtained at $\theta = 0°$ and $c = 0$.

formed again. On the other hand, comparison of R_g/R_h values at $S/P = 0.7$ suggests that the CPPSS complex with the highest amount of bound surfactant that is still soluble in water (i.e., just prior to precipitation) is more permeable for the solvent if it is composed of longer polyion chains, whereas shorter chains form more compact aggregates. A possible reason for this difference between short- and long-chain complexes may be a temporary network-like association of long polyion chains with sufficiently reduced charge due to the bound surfactant. When a short polymer chain collapses around a micelle, the remaining (free) part of the chain is not able to make entanglements, whereas in complexes with longer polymer chains this is possible and surfactant micelles serve as cross-links for the formation of a rather loose temporary network. The forces responsible for such labile intermolecular association are weak, in contrast to strong specific interaction involved in the formation of the primary complex between the PSS^- chain and surfactant micelle, and result in a more solvent-permeable structure. The apparent decrease in the density of the CPPSS-H particles formed when $S/P > 0.5$ is thus a clear sign of their nonspherical shape and/or inhomogeneous distribution of CPPSS-H material within the particle of radius R_g.

Under the described circumstances one might expect the occurrence of secondary multichain aggregates. However, we did not observe bimodal size distributions for CPPSS-H complexes even at $S/P = 0.7$ at any scattering angle. The observed size distributions of the CPPSS-H complex were monomodal and fairly narrow. However, the distributions at $S/P = 0.7$ were broader than those at $S/P = 0.5$ and the deviation of the Γ vs q^2 dependency from linearity was stronger. This supports the temporal and irregular character of structures of CPPSS-H.

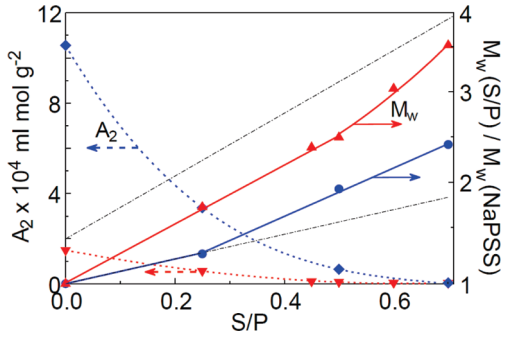

Figure 6. Dependence of the second virial coefficient, A_2 (dashed lines), and of the molar mass ratio, M_w(CPPSS)/M_w(NaPSS), on the S/P ratio (solid lines): CPPSS-L (blue symbols) and CPPSS-H (red symbols). The dashed−dotted lines show calculated trend of the M_w(CPPSS)/M_w(NaPSS) ratio for the case of CPPSS complexes that involve either one (lower line) or two (upper line) polyion chains.

Figure 6 visualizes the effect of the increasing S/P ratio on M_w and A_2 for both CPPSS complexes. The molar mass values are plotted as relative values, i.e., ratios of the molar mass of the corresponding NaPSS sample and of its complex with CP^+, M_w(CPPSS)/M_w(NaPSS). The M_w(CPPSS) values in this ratio were calculated using eq 3 by taking into account the degree of polymerization of the respective polyion and the average molar mass of the monomer unit, M_{PSC}, at a specified S/P value. This calculation of M_w considers only one polyion chain in the complex. Clearly, a larger M_w is obtained by taking into account the possibility of two polyion chains participating in complex formation. Both calculated trends are included in Figure 6 as dashed−dotted lines and fit the expected linear dependence of M_w(CPPSS)/M_w(NaPSS) on S/P. As can be seen, the experimental M_w values increase faster than one can expect if only one polymer chain interacts with CP^+ micelles. On the other hand, the molar mass ratio grows slower than it would if multichain (e.g., two-chain) complexes were formed. The determined molar mass values actually lie between the "one-chain" and the "two-chain" CPPSS clusters. Only for the CPPSS-H complex with $S/P = 0.7$ is the M_w value approaching the case of a "two-chain" cluster. This agrees with the above proposed temporal nature of intermolecular aggregates that are quite labile and can merge or decompose easily. In the case of longer chains, the entanglements are more probable and the determined average molar mass is higher, whereas with shorter chains more compact aggregates are formed that are not inclined to well-expressed intermolecular association. For example, the molar mass of the CPPSS-L with $S/P = 0.25$ case still fits the "one-chain" cluster.

A possible interpretation of these findings is as follows. The stable CPPSS cluster is initially formed by surfactant binding to one PSS^- chain. The cluster is stabilized by the inclusion of the benzene rings into the surfactant micelle; a mixed micelle is formed. Since PSS^- induced CP^+ micelles are comparatively small (see the aggregation numbers reported in the Introduction) and their interior is presumably rather "crowded" due to the described specific interaction, it may be difficult to accommodate two chains into one micelle. If incorporation of two (or more) PSS^- chains into the micelle is ruled out, intermolecular clusters can form only as a result of collisions and eventual hydrophobic interactions between complexes. Unless the overall charge of the complex is rather low, these events are rare and do not result in a permanent association, and

dx.doi.org/10.1021/jp2008336 |J. Phys. Chem. B XXXX, XXX, 000–000

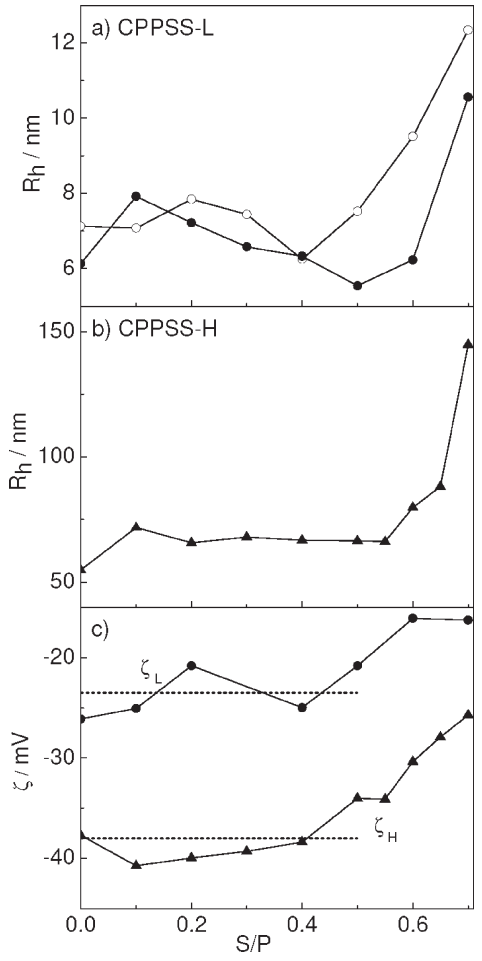

Figure 7. Dependence (a and b) of the apparent hydrodynamic radius, R_h, and (c) of the ζ-potential of CPPSS-L (ζ_L) and CPPSS-H (ζ_H) complexes on the S/P ratio. The concentration of NaPSS-L was 6.18 mg/mL (0.03 mol of monomer/L) and that of NaPSS-H was 2.06 mg/mL (0.01 mol of monomer/L). R_h^{app} was measured at θ = 173°. For comparison, R_h^{app} measured at θ = 90° by DLS is also presented (open circles). The dashed lines in the ζ vs S/P plot indicate the average ζ-potential values in the region S/P < 0.5 (see text).

the above conclusions on lability of intermolecular complexes become reasonable.

ζ-Potential of the CPPSS Complexes. In contrast to LS studies, the ζ-potential measurements were conducted at a constant polyion concentration. This means that the weight concentration of PSC solutions (in milligrams per milliliter) was increasing with increasing S/P, whereas the monomolar concentration was constant. The obtained results are shown in Figure 7. The R_h^{app} values of CPPSS-L complexes were measured before and after the ζ-potential and they agreed within the experimental error, showing that the effect of external electric field on particle size is negligible. Accordingly, all data reported for R_h^{app} in Figure 7 are those determined by the Zetasizer before the measurement of ζ-potential.

The size of both complexes in the region S/P < 0.5 is more or less constant, but increases for S/P > 0.5. This seems to be in contradiction to Figure 5, where R_h (values extrapolated to θ = 0!) decreases with increasing S/P. However, one should keep in mind that measurements shown in Figure 7 were performed with the Zetasizer at θ = 173° and at a finite polyelectrolyte concentration (no extrapolations to zero angle and zero concentration were carried out), and thus the obtained dimensions are apparent values that are affected by intermolecular association at finite concentrations. For comparison, R_h^{app} measured by DLS for CPPSS-L at θ = 90° at a comparable polyion concentration is also presented in Figure 7. Note also that the angular dependence becomes more pronounced for S/P values above 0.5, where solvent quality becomes poorer and the size distributions broaden.

Below $S/P \approx 0.5$, the ζ-potential of both complexes is around −23.5 and −38 mV for CPPSS-L and CPPSS-H, respectively, and decreases to around −15 and −27 mV at S/P = 0.7. The observation on the constancy of ζ-potential in a rather broad S/P region can be rationalized by taking into account the Manning counterion condensation theory.[42,43] According to this theory, the condensation of counterions to the polyion takes place if the linear charge density parameter, λ ($=ne_0/(4\pi\varepsilon\varepsilon_0 kTL)$, where n is the average degree of polymerization of the polyion, L is its extended chain length, and ε and ε_0 are the dielectric constant of the solvent and the permittivity of vacuum; the length of the monomer unit bearing an elementary charge e_0 is $b = L/n$, and ne_0 is the average value of the total polyion charge), of the polyion exceeds a certain critical value, λ_{crit}, thus keeping the effective polyion charge constant. For monovalent counterions, λ_{crit} is equal to 1,[42,43] and from this the critical spacing between charges on the polyion, b_{crit}, is b_{crit} = 0.72 nm. In the case of weak polyelectrolytes (e.g., polyacrylates), the distance between charges on the chain can be easily varied by changing the degree of ionization, α, of carboxyl groups. For a completely ionized vinyl polyelectrolyte (e.g., poly(styrenesulfonate) or polyacrylate with α = 1), the structural value of b is 0.276 nm. A simple calculation shows that b_{crit} = 0.72 nm (or λ_{crit} = 1) is achieved with $\alpha \approx 0.38$. Thus, for α > 0.38 counterions from solution (the Na^+ ones that are in large excess) will condense on the polyion and its effective charge will be kept constant (independent of α), whereas for α < 0.38 no counterion condensation will occur and thus the polyion charge will be determined by the value of α. A parallel parameter to α (the fraction of ionized or charged groups) in the case of CPPSS complexes is the quantity $1 - S/P$, which also equals the fraction of charged, i.e., free, groups on the polyion; these are the sulfate groups that are not blocked by bound surfactant ions.[11] Therefore, according to Manning theory the effective polyion charge and consequently also the ζ-potential should remain constant up to $1 - S/P \cong 0.38$ or $S/P \cong 0.62$, which satisfactorily agrees with the data in Figure 7. In agreement with our results, the electrophoretic mobility of DNA complexes with DTAB also was constant almost up to the saturation point.[26]

Finally, Figure 7 shows that the ζ-potential is more negative for CPPSS-H complexes. In the region of S/P values below 0.5, an average value of the ratio ζ_H/ζ_L is around 1.62 (calculated from −23.5 and −38 mV for CPPSS-L and CPPSS-H, respectively). The ζ-potential depends on the particle charge and size through $\zeta = ne_0/(4\pi\varepsilon\varepsilon_0 R_g)$, where R_g is the radius of a spherical colloidal particle.[44a] Thus, the ratio ζ/λ is equal to kTL/R_g. Since L scales proportionally with n ($L \propto n$) and R_g scales with n to a certain power ($R_g \propto n^x$; e.g., x = 0.5 for coils[44b]), ζ should be chain length dependent, as demonstrated also by the experimental values in Figure 7.

An estimation of the ratio ζ_H/ζ_L can be obtained also from dimensions measured by LS by taking into account $\zeta_H/\zeta_L = (R_{g,L}L_H)/(R_{g,H}L_L)$ (here it was assumed that the structural value of the linear charge density parameter λ does not depend on the

dx.doi.org/10.1021/jp2008336 |J. Phys. Chem. B XXXX, XXX, 000–000

chain length, i.e., $\lambda_H = \lambda_L$). By inserting the experimental R_g values obtained by LS for the complexes with $S/P = 0.5$ ($R_{g,L}$ and $R_{g,H}$ for short- and long-chain complexes, respectively) and the calculated average values of the extended lengths (L_L and L_H for short and long PSS chains, respectively), a value $\zeta_H/\zeta_L = 1.52$ is obtained, which is in good correspondence with the average value of this ratio determined directly from the measured ζ-potentials (see above).

CONCLUSIONS

A detailed static and dynamic light scattering study accompanied by ζ-potential measurements was performed on soluble polyelectrolyte−surfactant complexes of an anionic polyelectrolyte sodium poly(styrenesulfonate), NaPSS, and a cationic surfactant cetylpyridinium chloride, CPC, in aqueous NaCl solutions for two polyions with considerably different chain lengths. The particular system is characterized by the solubilization of the benzene rings in the hydrophobic micellar interior. This specific interaction leads to the fact that CPPSS complexes are perfectly soluble in 0.1 M NaCl up to a value of the surfactant-to-polyion charge ratio, S/P, close to 0.72, in strong contrast with other related systems. The S/P value at the onset of precipitation does not depend on the polyion chain length, and the phase separation (precipitation) is a fast process. Consequently, the stoichiometric CPPSS complex is easily dissolved in water or aqueous NaCl by adding excess NaPSS.

The R_h distributions of CPPSS particles in the polyelectrolyte-rich region are monomodal and moderately broad. The size parameters, R_h and R_g, decrease while molar mass, M_w, increases with increasing S/P, and simultaneously the second virial coefficient, A_2, decreases. These results point to strong contraction/compaction of the polyion chain, parallel to the case of DNA compaction by cationic surfactants, a subject deserving much attention recently. As revealed by ζ-potential data, this reduction in particle size occurs without significant changes in the effective charge of the complexes. CPPSS complexes adopt the smallest hydrodynamic radius at $S/P \approx 0.5$. Just prior to precipitation, the CPPSS complexes with shorter polyion chains are close to a spherical shape and are rather compact, whereas the ones with longer polyion chains are less compact and more inclined toward intermolecular association. However, the emerging associates are rather labile in nature and do not even influence the particle size distributions.

The easy dissolution of the stoichiometric CPPSS complex by adding excess polyelectrolyte is opposed with the situation in the surfactant-rich regime. Here, a large excess of surfactant and long dissolution times are required to achieve the redissolution of the precipitated complex. The process depends strongly on the polyion size. The explanation is again offered by the specific interaction, strongly marking this system. Due to this feature, the primary CPPSS complex is extremely stable and incorporation of more than an equivalent amount of surfactant into this structure is disfavored, as is its withdrawal from the complex. Consequently, free CPC micelles are first formed in solution that is in equilibrium with the precipitated CPPSS complex and only a large surplus of CPC leads to additional hydrophobic binding to the complex and its dissolution. An important additional consequence of the specific interaction between the PSS^- anion and the surfactant micelle is that the decomposition of the stoichiometric CPPSS complex into free polyion chains and free surfactant micelles requires very high NaCl concentrations as well.

As a final remark it is worthwhile to note that our studies do not indicate any extensive and stable intermolecular association into long-lived structures beyond the level of the primary PSCs in these solutions, at least not in the concentration regime probed by light scattering, although the nominal charge of the primary complexes is rather low. The strong initial interaction between the PSS^- anion and the CP^+ micelle is the origin of the exceptional solubility of the primary complex in the polyelectrolyte-rich regime ($S/P < 1$) and also of its difficult redissolution in the surfactant-rich regime ($S/P > 1$). In the polyelectrolyte-rich regime only nonstoichiometric PSCs are present in solution, whereas in the surfactant-rich regime the solubilized complexes coexist with a large excess of surfactant micelles. Additional intriguing questions now present themselves as to how these structures and the phase diagram in solutions of the PSS^- anion and a cationic surfactant evolve at higher solute concentrations. This is a subject of separate research.

ASSOCIATED CONTENT

Supporting Information. Detailed aspects of the data analysis, examples of data treatment, and additional experimental results. This material is available free of charge via the Internet at http://pubs.acs.org.

AUTHOR INFORMATION

Corresponding Author

*Tel.: +(386-1)-2419-412. Fax: +(386-1)-2419-425. E-mail: ksenija.kogej@fkkt.uni-lj.si.

Notes

[§]Permanent address: Institute of Macromolecular Compounds, Russian Academy of Sciences, 199004, Bolshoj pr., 31, St. Petersburg, Russia.

ACKNOWLEDGMENT

This work was financially supported by the Slovenian Research Agency, ARRS, through the Physical Chemistry program P1-0201. In addition, a great part of the experimental work has become possible thanks to the established bilateral agreement between the Academy of Finland (Grants 132404 and 134581) and the ARRS. The authors are also grateful to the ESF STIPOMAT program (Experimental and Theoretical Design of Stimuli-Responsive Polymeric Materials) for the financial support of the research visits (Grants 2294, 2603, 3030).

REFERENCES

(1) *Interactions of Surfactants with Polymers and Proteins*; Goddard, E. D., Ananthapadmanabahn, K. P., Eds.; CPC Press: Boca Raton, FL, USA, 1993.

(2) *Polymer-Surfactant Systems*; Kwak, J. C. T., Ed.; Surfactant Science Series 77; Marcel Dekker: New York, 1998.

(3) Piculell, L.; Lindman, B. *Adv. Colloid Interface Sci.* **1992**, *41*, 149–178.

(4) Piculell, L.; Svensson, A.; Norrman, J.; Bernardes, J. S.; Karlsson, L.; Loh, W. *Pure Appl. Chem.* **2007**, *79*, 1419–1434.

(5) Thalberg, K.; Lindman, B. *J. Phys. Chem.* **1989**, *93*, 1478–1483.

(6) Illekti, P.; Piculell, L.; Tournilhac, F.; Cabane, B. *J. Phys. Chem. B* **1998**, *102*, 344–351.

(7) Škerjanc, J.; Kogej, K.; Vesnaver, G. *J. Phys. Chem.* **1988**, *92*, 6382–6385.

(8) Škerjanc, J.; Kogej, K. *J. Phys. Chem.* **1989**, *93*, 7913–7915.
(9) Škerjanc, J.; Kogej, K. In *Macroion Characterization. From Dilute Solutions to Complex Fluids*; Schmitz, K. S., Ed.; ACS Symposium Series 548; American Chemical Society: Washington, DC, 1994; Chapter 20, pp 268−275.
(10) Kogej, K.; Škerjanc, J. Surfactant Binding to Polyelectrolytes. In *Physical Chemistry of Polyelectrolytes*; Radeva, T., Ed.; Surfactant Science Series 99; Marcel Dekker: New York, 2001; Chapter 21, pp 793−827.
(11) Kogej, K. *Adv. Colloid Interface Sci.* **2010**, *158*, 68–83.
(12) Kogej, K.; Škerjanc, J. *Langmuir* **1999**, *15*, 4251–4258.
(13) Gao, Z.; Kwak, J. C. T.; Wasylishen, R. E. *J. Colloid Interface Sci.* **1988**, *126*, 371–376.
(14) Andersson, M.; Rasmark, P. J.; Elvingson, C.; Hansson, P. *Langmuir* **2005**, *21*, 3773–3781.
(15) Hansson, P.; Jönsson, B.; Ström, B.; Söderman, O. *J. Phys. Chem. B* **2000**, *104*, 3496–3506.
(16) Hansson, P.; Almgren, M. *Langmuir* **1994**, *10*, 2115–2124.
(17) Balamenou, I.; Bokias, G. *Langmuir* **2005**, *21*, 9038–9043.
(18) Guillot, S.; Delsanti, M.; Désert, S.; Langevin, D. *Langmuir* **2003**, *19*, 230–237.
(19) Cardenas, M.; Schillen, K.; Nylander, T.; Jansson, J.; Lindman, B. *Phys. Chem. Chem. Phys.* **2004**, *6*, 1603–1607.
(20) Zhou, S.; Xu, C.; Wang, J.; Golas, P.; Batteas, J.; Kreeger, L. *Langmuir* **2004**, *20*, 8482–8489.
(21) Wang, C.; Tam, K. C. *J. Phys. Chem. B* **2004**, *108*, 8976–8982.
(22) Naderi, A.; Claesson, P. M.; Bergström, M.; Dedinaite, A. *Colloids Surf., A* **2005**, *253*, 83–93.
(23) Xia, J.; Zhang, H.; Rigsbee, D. R.; Dubin, P. L.; Shaikh, T. *Macromolecules* **1993**, *26*, 2759–2766.
(24) Li, Y.; Xia, J.; Dubin, P. L. *Macromolecules* **1994**, *27*, 7049–7055.
(25) Fundin, J.; Brown, W. *Macromolecules* **1994**, *27*, 5024–5031.
(26) Gorelov, A. V.; Kudryashov, E. D.; Jacquier, J. C.; Dawson, K. A. *Physica A* **1998**, *249*, 216–225.
(27) Villetti, M. A.; Borsali, R.; Crespo, J. S.;; et al. *Macromol. Chem. Phys.* **2004**, *205*, 907–917.
(28) Dias, R. S.; Pais, A. A. C. C.; Miguel, M. G.; Lindman, B. *Colloids Surf., A: Physicochem. Eng. Aspects* **2004**, *250*, 115–131.
(29) Lin, S. C.; Lee, W. I.; Schurr, J. M. *Biopolymers* **1978**, *17*, 1041–1064.
(30) Sedlak, M. *Macromolecules* **1993**, *26*, 1158–1162.
(31) Sedlak, M. *Langmuir* **1999**, *15*, 4045–4051.
(32) Cong, R.; Temyanko, E.; Russo, P.; Edwin, N.; Uppu, R. M. *Macromolecules* **2006**, *39*, 731–739.
(33) Schärtl, W. *Light Scattering from Polymer Solutions and Nanoparticle Dispersions*; Springer Verlag: Berlin, Heidelberg, 2007.
(34) Brown, W. *Dynamic Light Scattering: The Method and Some Application*; Clarendon Press: Oxford, 1993.
(35) Chu, B. *Laser Light Scattering: Basic Principles and Practice*; Academic Press: Boston, 1991.
(36) Urban, C.; Schurtenberger, P. *J. Colloid Interface Sci.* **1998**, *207*, 150–158.
(37) http://s-provencher.com/index.shtml (accessed Jan 26, 2011).
(38) *Polymer Handbook*; Brandrup, J., Immergut, E. H., Grulke, E. A., Abe, A., Bloch, D. R., Eds.; John Wiley & Sons, Inc.: New York, 1999.
(39) Borochov, N.; Eisenberg, H. *Macromolecules* **1994**, *27*, 1440–1445.
(40) Goddard, E. D. *Colloids Surf.* **1986**, *19*, 255–300. Leung, P. S.; Goddard, E. D.; Han, C.; Glinka, C. J. *Colloids Surf.* **1985**, *13*, 47–62.
(41) Leung, P. S.; Goddard, E. D.; Han, C.; Glinka, C. J. *Colloids Surf.* **1985**, *13*, 47–62.
(42) Manning, G. S. *J. Chem. Phys.* **1969**, *51*, 924–933.
(43) Manning, G. J. S. *Q. Rev. Biophys.* **1978**, *2*, 179–179.
(44) (a) Hunter, R. J. *Foundations of Colloid Science*; Clarendon Press: Oxford, 1987; Vol. 1. (b) Evans, F. D.; Wenerstrom, H. *The Colloidal Domain: Where Physics, Chemistry, Biology and Technology Meet*, 2nd ed.; Wiley-VCH: New York, 1999.